

## TRANSFER PROCESSES IN LOW-TEMPERATURE PLASMA

IN-LIQUID PLASMA RECYCLING METHOD  
OF ZINC OXIDE NANOPARTICLES

N. Amaliyah,<sup>a</sup> I. Rahim,<sup>b</sup> A. E. Eka Putra,<sup>a</sup>  
S. Mukasa,<sup>c</sup> S. Nomura,<sup>c</sup>  
and H. Toyota<sup>c</sup>

UDC 533.9

*Zinc nanoparticles applied in the production of zinc–air batteries provide the highest specific energy among various metal–air combinations used in batteries in practice. Recent technical advances provide an opportunity to successfully solve the problems experienced during the early development of batteries of this type. For example, there is a major limitation in recharging cycles due to the massive formation of zinc oxide. In the present work, a reduction process is proposed on the basis of the use of alcohol solvent by applying microwave in-liquid plasma. The occurrence of reduction was confirmed by calculating the chemical potential of ethanol and methanol as well as spectra of plasma emission in the temperature range 1500–2000 K. Characterization of synthesized nanoparticles was carried out by energy-dispersive X-ray spectrometry and transmission electron microscopy.*

**Keywords:** zinc nanoparticles, in-liquid plasma, alcohol solvent, reduction, microwave plasma.

**Introduction.** Increasing demand for oil and a limitation on nonrenewable energy resources as well as the effects of global warming have forced us to consider alternative energy storage and conversion systems. Recently, nanostructured materials have attracted attention in connection with their application in energy storage systems, especially in those with desirable charge/discharge rates, such as batteries [1, 2]. Zinc–air batteries become an attractive option due to their beneficial characteristics, such as high-energy density, low cost, and environmental benignity. However, the formation of a large quantity of zinc oxide along with issues concerning its recycling are somewhat problematic from a commercial point of view for the development of rechargeable zinc–air batteries in practice.

In the synthesis of ZnO quantum particles, nucleation and growth occur rapidly in the presence of longer-chain alcohol [3]. By the sonochemical method, H<sub>2</sub>PtCl<sub>6</sub> was reduced to platinum (Pt) nanoparticles when using methanol as a solvent, while agglomerated Pt nanoparticles were synthesized with ethanol [4]. Platinum nanoparticles and nanorods were also synthesized by the microwave-assisted solvothermal techniques with methanol and ethanol as both reducing agents and solvents [5]. The UV pulsed laser irradiation of iron powder in methanol solves iron oxide nanowires, and iron nanoparticles are obtained by using ethanol, isopropanol, and glycol [6].

Alcohol, due to its nontoxicity and harmless to the environment, has been used as a reductant for the synthesis of many metal nanoparticles, such as platinum [4, 5], silver [7, 8], graphene [9], zinc oxide [3, 10], titania [11, 12], iron oxide [6], and copper [13], and these are just a few of them. Combining alcohols with efficient heating will intensify the reduction reaction. In-liquid plasma is suitable for generating high temperatures. Moreover, when plasma and an alcoholic solvent are applied, the oxidative or reductive atmosphere of a vapor of a liquid makes it possible to determine the physical properties of the nanoparticles synthesized.

Zinc and zinc nanoparticles are synthesized from zinc electrodes by applying in-liquid plasma generated by microwave radiation with a power of 250 W [14]. In a previous study, cubic and hexagonal zinc nanoparticles were synthesized by microwave (2.45 GHz) in-liquid plasma through reduction of zinc oxide with the use of ethanol as a reducing

---

<sup>a</sup>Department of Mechanical Engineering, Hasanuddin University, Gowa, 92171, Indonesia; email: novriany@unhas.ac.id; <sup>b</sup>Department of Automotive Technology Vocational Education, State University of Makassar, 90224, Indonesia; <sup>c</sup>Graduate School of Science and Engineering, Ehime University, Matsuyama, 790-8577, Japan. Published in *Inzhenerno-Fizicheskii Zhurnal*, Vol. 94, No. 6, pp. 1501–1506, November–December, 2021. Original article submitted June 20, 2020; revision submitted January 23, 2021.

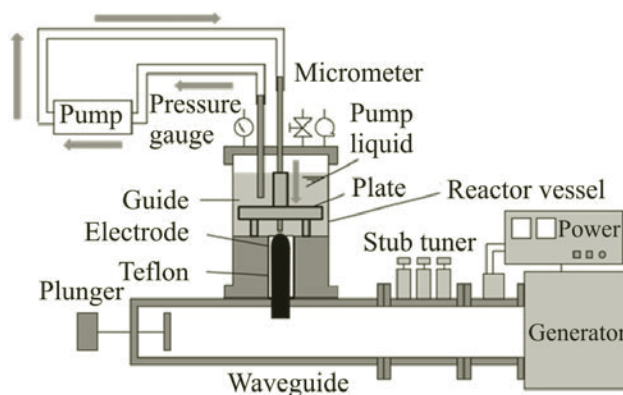


Fig. 1. Experimental apparatus.

agent. A decrease in the oxygen to zinc mass ratio was confirmed, although some residual oxide was observed [15]. To achieve perfect reduction, the desired type of solvent and the appropriate temperature should be selected.

The objectives of the present work are to study the recycling method of zinc oxide nanoparticles with the use of ethanol and methanol as reducing agents and to determine the influence of an alcoholic solvent on the oxide reduction.

**Experimental Method.** The experimental apparatus and methodology for generating MW (microwave) in-liquid plasma primarily conforming to those used in [15] are directed to increased efficiency. A schematic view of the experimental apparatus is shown in Fig. 1. A coaxial electrode fixed to the bottom of the reactor vessel is composed of a copper inner electrode 10 mm in diameter with a hemispherical Teflon-wrapped tip and a brass outer electrode. At the bottom of the vessel, polycarbonate at an angle of  $60^\circ$  used in [15] is replaced with an aluminum plate 39 mm in diameter with a tiny hole at the center placed above the tip of the coaxial electrode. On addition of the plate, the plasma emission became stronger for the naked eye and continued continuously as the gap between the plate and the coaxial electrode was filled with vapor [16]. A copper tube with an outer diameter of 3 mm and an inner diameter of 2 mm used as a counter electrode was placed at 1 mm from the coaxial electrode.

ZnO powder labeled 200 mesh (99.999%, NEWMET KOCH) was used. This powder weighting 0.3 g was dissolved in 120 ml of ethanol and methanol. The mixture was agitated with the use of an ultrasonic device until the powder was dispersed sufficiently. This liquid was poured into the vessel, and then the pressure was decreased to 30 kPa with the use of an aspirator. The liquid circulated by the action of a gear pump and coursed from the counter electrode toward the top of the inner electrode.

By adjusting a plunger and stub tuner, the input power was brought to 400 W until plasma irradiation occurred between the coaxial and counter electrodes. The plasma emission spectrum was measured by a spectroscope (PMA-11 HAMAMATSU), while the synthesized materials were identified by an energy-dispersive X-ray spectrometer (EDS) as well as by observation with the use of a transmission electron microscope (TEM) (JEM-2100, JEOL).

**Results and Discussion.** From calculating the chemical potential of ethanol and methanol, the reduction of ZnO is predicted by a consideration of chemical equilibrium. The thermal equilibrium composition of dominant products on reaction of zinc oxide with ethanol and methanol was calculated from the JANAF Thermodynamic Tables. The change in the Gibbs energy of zinc oxidation indicates that the reduction of the environment occurs at temperatures above 1140 K [15]. As shown in Fig. 2, at a temperature of about 1140 K, the dominant products are hydrogen and carbon monoxide. A greater proportion of CO is required for the oxide reduction. At this temperature, oxygen starts to release and bind to CO and  $H_2$ , so the production of  $H_2O$  and  $CO_2$  increases. At approximately 1900 K, the mole fractions of  $CO_2$  and  $H_2O$  decrease. Oxide reduction is considered to develop continuously within this temperature range because the mole fraction of  $O_2$  increases, whereas the mole fractions of  $H_2O$  and  $CO_2$  decrease.

Ethanol and methanol themselves can be energy sources. The changes in the total enthalpy of these solvents for the reduction of 1 mole of ZnO are shown in Fig. 3. The theoretical value of the enthalpy for the reduction of ZnO is 348.3 kJ. For ethanol at the temperature 1150 K, the enthalpy change is 388 kJ, which is higher than the theoretical value. Because the dominant products with the use of ethanol are hydrogen, carbon monoxide, and solid carbon, the total enthalpy is higher than that of ethanol. At a temperature between 1500 and 2000 K, the enthalpy change becomes less than 348.3 kJ with a minimum of 144 kJ.

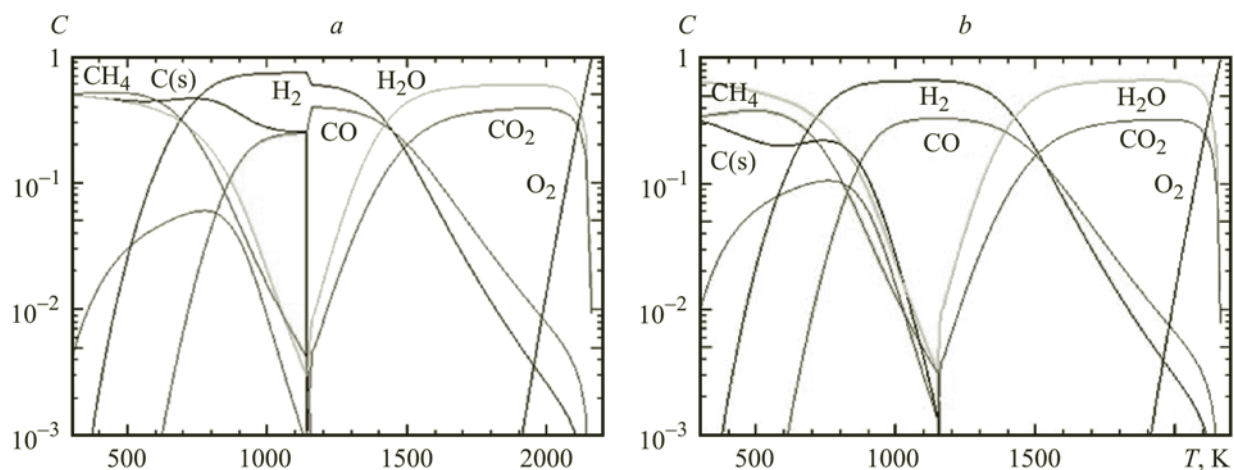


Fig. 2. Mole fraction for thermal equilibrium for methanol (a) and ethanol (b).

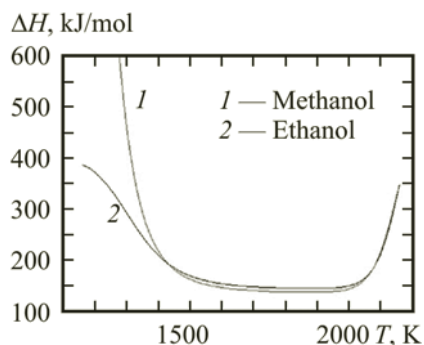


Fig. 3. Required enthalpy vs. the temperature.

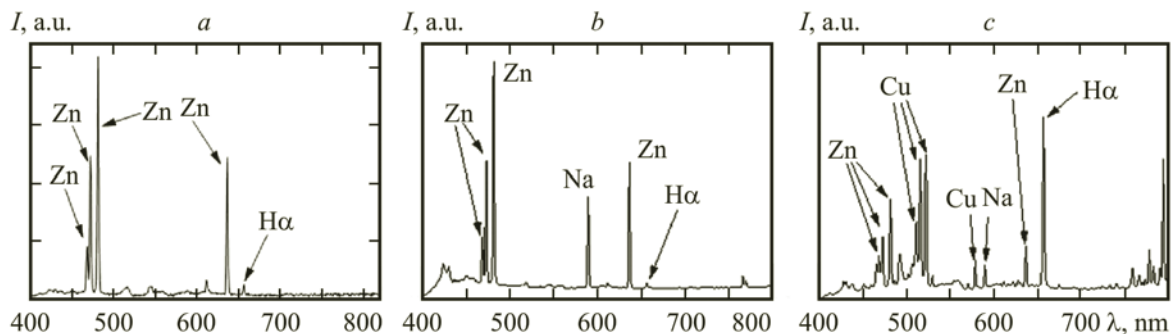


Fig. 4. Spectra of plasma emission for ethanol (a), methanol (violet) (b), and ethanol (blue-white) (c).

The same tendency is shown when applying methanol as a reducing agent. The required enthalpy decreases as the temperature increases to 1400 K with low enthalpy values occurring at 1500–2000 K. It is assumed that the reduction reaction takes place in this area. Methanol has a lower required enthalpy than ethanol. It is assumed that the enthalpy needed to reduce oxygen increases with the number of carbons in alcohol. When alcohol acts as a reducing agent, some covalent bonds are broken and a new bond is formed. As this takes place, more energy is released which then is absorbed, breaking alcohol bonds.

By applying the input power 400 W, plasma was generated for around 10 min. When ethanol was used, violet plasma emission was visible to the naked eye, and in the case of methanol, violet and blue-white emissions were observed.

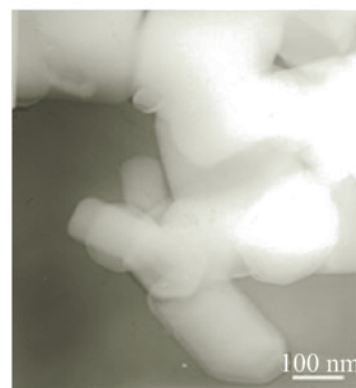
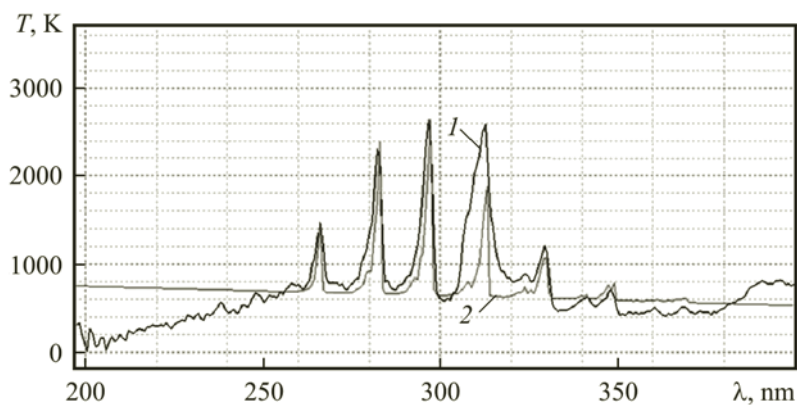


Fig. 5. Experimental (1) for 3.1597 nm and calculated (2) for 1.7484 nm spectral bands of CO.

Fig. 6. TEM image of nanopar-ticles obtained in methanol.

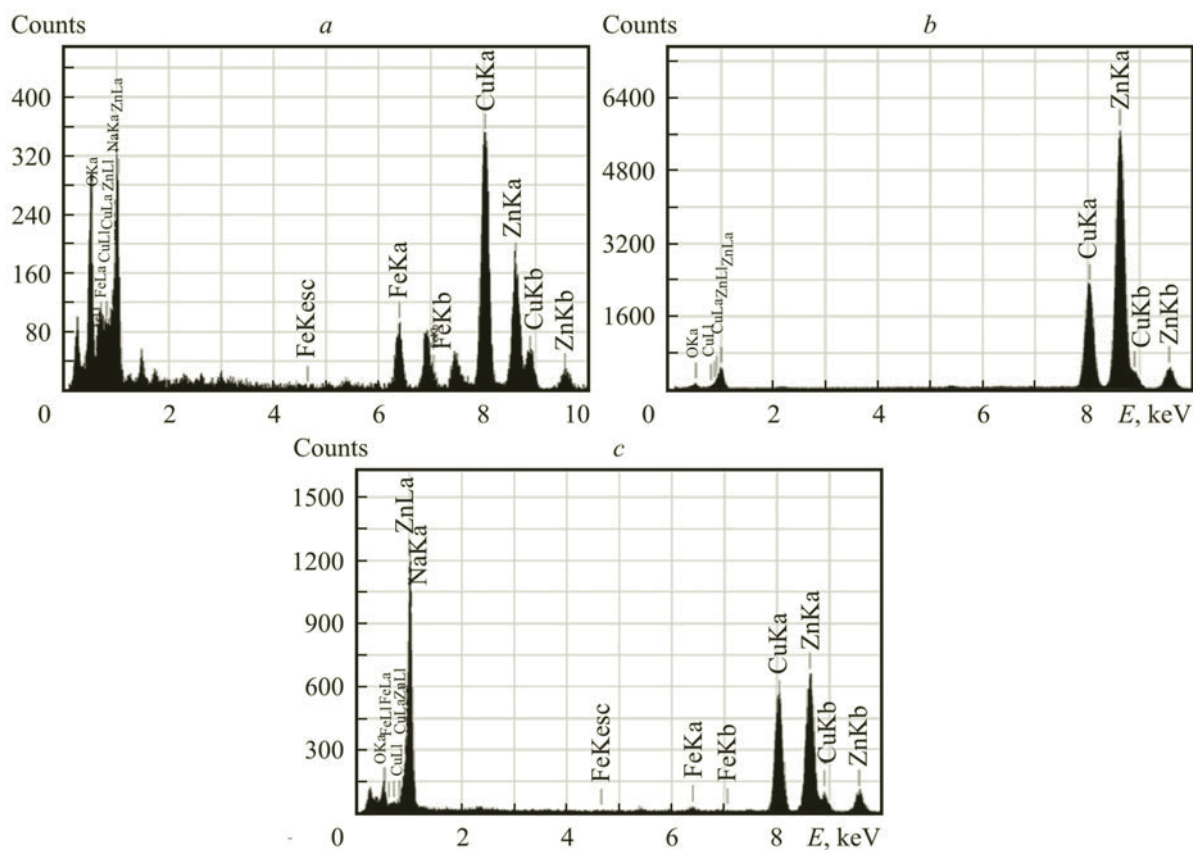


Fig. 7. EDS spectra of liquid obtained before plasma irradiation (a) and after plasma irradiation in ethanol (b) and in methanol (c).

Spectroscopic measurements were carried out by a PMA-11 C7473 (Hamamatsu) spectroscope to determine the emission spectra for both ethanol and methanol. Figure 4a shows the emission spectrum in the case of ethanol with characteristic lines for zinc detected at 468.0, 472.2, 481.1, and 636.2 nm. The same peak was also observed for violet emission in the case of methanol, as shown in Fig. 4b, where the H $\alpha$  peak occurs at 656 nm. This H $\alpha$  peak then becomes higher (see Fig. 4 c), which is the reason for the change in the plasma emission color from violet to blue-white.

From the theoretical analysis of thermal equilibrium it follows that oxygen reduction demands an appropriate temperature in the range 1500–2000 K. It was shown that reducing ZnO by silicon is thermodynamically possible at temperatures between 1100 and 1500 K [17]. The reduction of ZnO with the use of CO shows a strong temperature dependence in the range 1183–1497 K [18]. A spectrum simulation program was applied to calculate the spectral line at various temperatures as well as for comparison with a spectrum obtained from the experiment. Figure 5 shows the CO spectral band observed in plasma emission at 250–350 nm (here the values in the legend correspond to the spectral lines of ZnO). The rotational and vibration temperatures can be attained by matching the configuration of the spectral band to that from the computational simulation. There is good agreement with the measured value at 1600 K. Since this temperature is within the range of the theoretical results, it is believed that in-liquid plasma provides a reducing environment for oxide.

After plasma irradiation, the produced nanoparticles were examined by a transmission electron microscope (TEM, 200 KV, JEOL, JEM-2100). The ZnO nanoparticles used throughout this study were a mixture of rectangular and hexagonal ones 50–200 nm in length before plasma irradiation [15]. The change in the nanoparticle shape was not confirmed after plasma irradiation either in ethanol or in methanol, as shown in Fig. 6. The size 100 nm of rectangular particles was observed in ethanol, which is similar to previous results [15]. For methanol, particle aggregation was remarkable in the remaining liquid. However, agglomeration phenomena have not been confirmed yet.

Despite no significant difference for particles synthesized after plasma irradiation, hardly any oxygen is detected in comparison to its amount before irradiation. From the energy dispersive X-ray spectrometry (EDS) results, the oxygen to zinc mass ratio decreased from 24% before plasma irradiation (Fig. 7a) to 6% after irradiation in ethanol (Fig. 7b) and 0.46% for methanol (Fig. 7c).

Several works on the zinc recovery have been presented. However, there is no information yet about its recovery in the nanoparticle sizes. With using carbon in the presence of various additives, gaseous zinc product and oxygen tend to recombine, resulting in the formation of ZnO, which further decreases the recovery efficiency [19, 20]. When methane is used as a reducing agent to recover zinc, the product which is also gaseous should be cooled down rapidly to separate it from a syngas [20, 21]. Nanoparticles produced by the in-liquid plasma method are dispersed in the remaining liquid. By evaporating the liquid, they can be collected easily. In addition, since the reaction area is separated from the air, reoxidation is avoided.

**Conclusions.** Zinc nanoparticles have been synthesized by the reduction of zinc oxide nanoparticles with the use of ethanol and methanol as solvents while applying microwave in-liquid plasma method. In this method, reduction takes place in the temperature range 1500–2000 K. The thermal equilibrium compositions of dominant products when zinc oxide reacts with ethanol and methanol and the spectrum of plasma emission confirmed that in-liquid plasma provided the oxide reduction. The change in the nanoparticle shape after plasma irradiation was not confirmed. However, the oxygen to zinc mass ratio decreased for both ethanol and methanol from 24% to 6% and 0.46%, respectively. Agglomerated particles were observed when employing methanol, though here the enthalpy required for the reduction is lower than that for ethanol. Thus these results open up promising potentialities for the reduction in the nanoparticle size. Despite the possibility for the oxide reduction by the in-liquid plasma method, it is necessary to carry out further investigations to determine the optimal reaction parameter and reduction mechanism.

## NOTATION

$C$ , mole fraction;  $E$ , energy, keV;  $I$ , intensity, a.u.;  $T$ , temperature, K;  $\Delta H$ , change in the total enthalpy, kJ/mol;  $\lambda$ , wavelength, nm.

## REFERENCES

1. J.-S. Lee, S. Tai Kim, R. Cao R, N.-S. Choi, M. Liu, K. Tae Lee, and J. Cho, Metal–air batteries with high energy density: Li–air versus Zn–air, *Adv. Energy Mater.*, **1**, No. 1, 34–50 (2011).
2. V. Caramia and B. Bozzini, Materials science aspects of zinc–air batteries: A review, *Mater. Renew. Sustain. Energy*, **3**, No. 2, 28–40 (2014).
3. Z. Hu, G. Oskam, and P. C. Searson, Influence of solvent on the growth of ZnO nanoparticles, *J. Colloid Interface Sci.*, **263**, No. 2, 454–460 (2003).
4. L. Obreja, N. Foca, M. I. Popa, and V. Melnig, Alcoholic reduction platinum nanoparticles synthesis by sonochemical method, *Biomater. Biophys., Medical Phys. Ecology*, No. 11, 31–36 (2008).

5. D. Li and S. Komarneni, Synthesis of Pt nanoparticles and nanorods by microwave-assisted solvothermal technique, *Z. Naturforsch.*, **5**, 1566–1572 (2006).
6. S. S. J. Mollaha, C. E. G. Henleyb, and S. R. P. Silvab, Photo-chemical synthesis of iron oxide nanowires induced by pulsed laser ablation of iron powder in liquid media, *Integr. Ferroelectr.: An Int. J.*, **119**, No. 1, 45–54 (2010).
7. D. O. Oseguera-Galindo, A. Martínez-Benítez, A. Chávez-Chávez, G. Gómez-Rosas, A. Pérez-Centeno, and M. A. Santana-Aranda, Effects of the confining solvent on the size distribution of silver NPs by laser ablation, *J. Nanoparticle Res.*, **14**, No. 9, 1133 (2012).
8. H. J. Hah, S. M. Koo, and S. H. Lee, Preparation of silver nanoparticles through alcohol reduction with organoalkoxysilanes, *J. Sol-Gel Sci. Technol.*, **26**, 467–471 (2003).
9. C. Gong, M. Acik, R. M. Abolfath, Y. Chabal, and K. Cho, Graphitization of graphene oxide with ethanol during thermal reduction, *J. Phys. Chem. C*, **116**, No. 18, 9969–9979 (2012).
10. P. Banerjee, S. Chakrabarti, S. Maitra, and B. K. Dutta, Zinc oxide nanoparticles – Sonochemical synthesis, characterization and application for photo-remediation of heavy metal, *Ultrason. Sonochem.*, **19**, No. 1, 85–93 (2012).
11. B. Liu, Y. Wang, Y. Huang, P. Dong, and S. Yin, Morphological control and photocatalytic activities of nitrogen-doped titania nanoparticles by microwave-assisted solvothermal process, *J. Aust. Ceram. Soc.*, **48**, 249–252 (2012).
12. D. Liang, C. Cui, H. Hu, Y. Wang, S. Xu, B. Ying, P. Li, B. Lu, and H. Shen, One-step hydrothermal synthesis of anatase TiO<sub>2</sub>/reduced graphene oxide nanocomposites with enhanced photocatalytic activity, *J. Alloys Compd.*, Issue 582, 236–240 (2014).
13. T. Nakamura, Y. Tsukahara, T. Sakata, H. Mori, Y. Kanbe, H. Bessho, and Y. Wada, Preparation of monodispersed Cu nanoparticles by microwave-assisted alcohol reduction, *Bull. Chem. Soc. Jpn.*, **80**, 1492–1503 (2007).
14. Y. Hattori, S. Mukasa, H. Toyota, T. Inoue, and S. Nomura, Synthesis of zinc and zinc oxide nanoparticles from zinc electrode using plasma in liquid, *Mater. Lett.*, **65**, No. 2, 188–190 (2011).
15. N. Amaliyah, S. Mukasa, S. Nomura, and H. Toyota, Plasma in-liquid method for reduction of zinc oxide in zinc nanoparticle synthesis, *Mater. Res. Express*, **2**, No. 2, 025004 (2015).
16. Y. Hattori, S. Nomura, S. Mukasa, H. Toyota, T. Inoue, and T. Kasahara, Synthesis of tungsten trioxide nanoparticles by microwave plasma in-liquid and analysis of physical properties, *J. Alloys Compd.*, Issue 560, 105–110 (2013).
17. C. Qi-Yuan, Thermodynamic analysis of silicothermic reduction zinc oxide in vacuum, *Acta Phys.-Chim. Sin.*, **27**, No. 6, 1312–1318 (2011).
18. G. Gonzalez, S. Jordens, and S. Escobedo, Dependence of zinc oxide reduction rate on the CO concentration in CO/CO<sub>2</sub> mixtures, *Thermochim. Acta*, **278**, 129–134 (1996).
19. B.-S. Kim, J.-M. Yoo, J.-T. Park, and J.-C. Lee, A kinetic study of the carbothermic reduction of zinc oxide with various additives, *Mater. Transact.*, **47**, No. 9, 2421–2426 (2006).
20. C. Wieckert and A. Steinfeld, Solar thermal reduction of ZnO using CH<sub>4</sub> : ZnO and C : ZnO molar ratios less than 1, *J. Solar Energy Eng.*, **124**, No. 1, 55–62 (2002).
21. H. A. Ebrahim and E. Jamshidi, Kinetic study of zinc oxide reduction by methane, *Chem. Eng. Res. Des.*, **79**, No. 1, 62–70 (2001).